Equation of state measurements in liquid deuterium to 100 GPa

2003 J. Phys. A: Math. Gen. 36 6149

(http://iopscience.iop.org/0305-4470/36/22/342)

INSTITUTE OF PHYSICS PUBLISHING JOURNAL OF PHYSICS A: MATHEMATICAL AND GENERAL

J. Phys. A: Math. Gen. **36** (2003) 6149–6158 PII: S0305-4470(03)54991-5

Equation of state measurements in liquid deuterium to 100 GPa

M D Knudson, D L Hanson, J E Bailey, R W Lemke, C A Hall, C Deeney and J R Asay

Sandia National Laboratories, Albuquerque, NM 87185-1181, USA

Received 18 October 2002, in final form 10 January 2003
Published 22 May 2003
Online at stacks.iop.org/JPhysA/36/6149

Abstract

Using intense magnetic pressure, a method was developed to launch flyer plates to velocities in excess of 20 km s^{-1}. This technique was used to perform plate-impact, shock wave experiments on cryogenic liquid deuterium (LD_2) to examine its high-pressure equation of state (EOS). Using an impedance matching method, Hugoniot measurements were obtained in the pressure range of 22–100 GPa. The results of these experiments disagree with the previously reported Hugoniot measurements of LD_2 in the pressure range above ∼40 GPa, but are in good agreement with first principles, *ab initio* models for hydrogen and its isotopes.

PACS numbers: 62.50.+p, 64.30.+t

1. Introduction

The high-pressure equation of state (EOS) of hydrogen and its isotopes has been the subject of considerable interest, principally due to the importance of the EOS to such areas as inertial confinement fusion, planetary astrophysics and our fundamental understanding of warm dense matter. Until recently, the most widely accepted EOS model was the Sesame model [1]. Prior to 1997, Hugoniot measurements of liquid hydrogen and deuterium had been limited to the pressure range below approximately 20 GPa [2], which is accessible by conventional gas-gun, plate-impact experiments. However, recent measurements from laser-driven experiments [3] at pressures of 20–300 GPa suggest that LD_2 is much more compressible than previously thought. The results from these laser-driven experiments suggest a maximum compression in excess of $\rho/\rho_0 = 6$, which deviates significantly from the Sesame EOS that predicts a maximum compression of approximately 4.4.

Despite efforts to model this apparent increase in compressibility, several theoretical models based on first principles, *ab initio* methods [4–6] are unable to describe the experimental results above ∼40 GPa. Rather, as the approximation schemes in these *ab initio* methods have improved, these models [4–6] have converged, yielding results that are

closer to the Sesame EOS at high shock pressures, and disagree with the phenomenological linear mixing model of Ross [7] that is in relatively good agreement with the laser-driven data. The inability to resolve this discrepancy has raised concern that either our understanding of the physics governing the EOS of these simple elements is lacking or there is a systematic error in the experiments.

Some of the concerns centre around the small sample sizes and the method used in the laser experiments to drive the shock wave. Considering the relatively high shock velocities and the extremely high sound speeds in the shocked state, the experimental measurements were made on a few nanoseconds timescale, which limited the overall accuracy of the EOS data. Furthermore, the use of ablatively driven shock waves raises concerns regarding the duration, planarity and constancy of the shock wave.

Given the significant discrepancy between theory and experiment, it is desirable to obtain independent EOS measurements of LD_2 with sufficiently different experimental techniques that are not subject to the limitations listed above, and that have the potential for increased accuracy. Recently, a new capability has been developed to isentropically compress materials to high pressures [8] using the intense magnetic pressure produced by the Sandia Z accelerator [9]. This new capability has been used to launch relatively large flyer plates to velocities about three times higher than that possible using conventional gas-gun technology. The flyer plate technique for performing high-pressure shock wave experiments is particularly attractive for several reasons. First, the experiments are plate-impact experiments, and thus produce a well-defined shock loading of the sample, with a substantial duration of constant pressure (to 30 ns). Second, relatively large sample diameters and thicknesses are possible, thus increasing the accuracy of the EOS data. Finally, the large sample sizes allow for multiple and redundant diagnostics to be fielded which further enhance the accuracy and confidence of the data.

2. Flyer plate technique

The flyer plates comprise the anode of a short circuit load at the centre of the Z accelerator. The interaction of the current density and magnetic field produced in the insulating gap results in a time-dependent pressure, $P(t)$, that is applied to the inner surface of the flyer plate. The magnitude of this loading is given by $P(t) = B^2/2\mu_0 = \mu_0 J^2(t)/2$. Here $J(t)$ is time-dependent current density (amps/unit length) at the sample location, B is the magnetic field strength and μ_0 is the magnetic permeability of free space. In the normal firing configuration for the accelerator, $J(t)$ increases approximately linearly over a $\sim$200 ns rise time. This impulsive, ramp load provides momentum to the anode and launches it as a flyer plate to high velocity.

Typically four aluminium anode panels are arranged about a central stainless steel cathode post, forming a symmetric anode–cathode gap. A short circuit is created between the anode panels and cathode post through a shorting cap at the top of the coaxial load. Each anode panel becomes a flyer plate; this is achieved by machining the entire current carrying portion of the aluminium anode panel to a prescribed material thickness of approximately 800–900 μm. To retain rigidity, and to allow the panels to be assembled together, the flyer frame is attached to a panel back. The panel back also allows for mounting of the experimental target at a prescribed distance from the flyer plate, which is typically $\sim$3 mm. An alternate configuration employs a thinner aluminium plate that acts as a driver to launch a separate, embedded titanium flyer. The current carrying surface of each panel and the impact surface of the flyer are flat to $\sim$200 nm and parallel to $\sim$2 μm with $\sim$20 nm surface finishes. Each of the panel backs can hold two

separate targets, allowing up to eight simultaneously shock wave experiments during a single firing of the accelerator.

The magnitude of the field, and thus the driving pressure pulse, can be adjusted by changing the geometry of the short circuit load, and thus the current density. Two typical short circuit geometries are a square coaxial geometry, in which four equal width anode panels surround a square cathode stalk, and a rectangular geometry, in which two of the sides of the square geometry are shrunk to roughly half the width. The square geometry produces a $\sim$1 Mbar driving pressure capable of launching up to four aluminium flyers to $\sim$16 km s^{-1} and up to four titanium flyers to $\sim$14 km s^{-1}. The rectangular or slab geometry, which increases the current density at the expense of two flyer plates, produces a $\sim$2.5 Mbar driving pressure capable of launching up to two aluminium flyers to $\sim$21 km s^{-1} and up to two titanium flyers to $\sim$22 km s^{-1}. Besides changing the short circuit geometry, the current density for a given geometry can also be lowered by reducing the charge voltage of the accelerator. Since the peak current scales approximately linearly with the charge voltage, the driving pressure can be reduced by as much as 50%. These two parameters, the geometry and the charge voltage, allow the flyer velocity to be varied essentially continuously over the range of $\sim$7–22 km s^{-1}.

To a very crude approximation the final velocity of the flyer can be estimated analytically by applying conservation of momentum, and treating the magnetic pressure pulse as an impulsive load, integrating over time to determine the total momentum transferred to the plate. However, due to the enormous field strength ($\sim$5–7 MG) and currents ($\sim$20 MA) associated with this technique, the details of the flyer plate launch are somewhat more complicated and cannot be approached through simple analytical measures. Computer simulations, which include all the experimental parameters and necessary physics, are required for more accurate velocity predictions [10].

To obtain a better understanding of the flyer plate launch, both one- and two-dimensional Eulerian simulations have been performed using the finite element, arbitrary Lagrangian–Eulerian, magneto-hydrodynamic (MHD) code ALEGRA [11]. MHD equations for a compressible material with material strength were solved. An EOS valid for a wide range of pressures ($P < 5$ Mbar), densities ($\rho < 50.0$ g cm^{-3}) and temperatures ($T < 10$ eV) was used for aluminium [12], in addition to models for the thermal and electrical conductivities[1] [13, 14]. Density and internal energy are used in the EOS to obtain pressure and temperature. The density and temperature are used in the conductivity model to obtain electrical and thermal conductivities. The form of Ohm's law used in ALEGRA is $\vec{J} = \sigma(\vec{E} + \vec{v} \times \vec{B})$, where $\vec{J}$ is the current density, σ is the electrical conductivity, $\vec{E}$ is the resistive electric field and $\vec{B}$ is the applied magnetic field. More details concerning the MHD modelling of flyer plate launch can be found elsewhere [10].

Results of the MHD simulations are in very good agreement with experiment, and have provided significant insight into the details of the flyer plate launch. In particular, the one-dimensional simulations allow us to predict the final flyer velocity for new short circuit configurations, as well as the state of the flyer plate just prior to impact. Simulations indicate that a significant portion of the original thickness of the flyer plate is vaporized due to Joule heating. For appropriate initial flyer thicknesses, approximately 200–300 μm of the impact side of the flyer remains at solid density. This Joule heating and subsequent magnetic field diffusion are what preclude the ability to approach this problem analytically. In particular,

[1] The electrical and thermal conductivity model used is a recent model by Desjarlais [13]. The model is similar to the Lee–More–Desjarlais (LMD) model [14]; however, *ab initio* calculations [15] indicated that the LMD model underestimated the conductivity of aluminium by $\sim$70% in the dense liquid regime and appropriate corrections to the LMD model were made. This new model has resulted in improved agreement in MHD simulations of wire expansion [16] and flyer plate experiments [10].

these simulations indicate that a significant fraction of the final velocity of the flyer is the result of ablation of the Joule heated material on the power-flow surface.

The two-dimensional simulations allow us to determine the extent of curvature of the flyer plate due to magnetic field gradients within the anode–cathode gap. Due to the two-dimensional nature of the square or rectangular short circuit load, magnetic pressure gradients across the horizontal direction of the flyer plate (perpendicular to the axis of the load) are unavoidable. The electromagnetic (EM) code QUICKSILVER [17] was used to determine the magnitude of the magnetic pressure gradients for the initial geometry of the anode and cathode. These simulations indicate that the magnetic pressure is uniform to better than 1% over the central 6 mm of the flyer plate. However, the pressure drops quite rapidly towards the corners of the cathode. These gradients will cause velocity variations across the flyer surface, leading to plate distortions. These distortions will amplify as the flyer is launched towards the target; the launching of plate deforms the anode–cathode gap, reducing the area over which the magnetic pressure is uniform. Independent of any edge effects, this process gives rise to velocity gradients within the flyer that result in curvature of the plate.

Predictions of the two-dimensional MHD simulations that account for the time-dependent deformation of the anode–cathode gap suggest that the central $\sim$4 mm width of the original 15 mm wide flyer remains quite planar. In contrast, the magnetic pressure gradient is rather independent of height along the flyer portion of the co-axial short circuit load. There are variations as a function of height near the transition of the cathode from a radial feed to a co-axial feed; however, the current density is quickly redistributed, and becomes quite uniform over the co-axial region of interest for these experiments. This suggests that there should be little to no curvature of the plate along the vertical direction; i.e., the curvature is limited to the horizontal direction. This is indeed what has been observed experimentally; at impact the flyer plate is quite planar over roughly 3–4 mm in the horizontal direction and extremely planar over the entire vertical direction.

The best indication of the constancy of pressure produced at impact by these magnetically accelerated flyers is from data obtained in the $L\mathrm{D}_2$ experiments [18]. These results, which indicate that the drive pressure remains constant to better than $\sim$1–2%, will be discussed in the following section.

3. Deuterium experiments

The experimental configuration used to obtain Hugoniot data with the magnetically driven impact technique is shown in figure 1. The necessary cryogenics were provided by an expendable cryocell connected to a survivable cyrostat [19]. The cavity of the cryocell was defined by a stepped aluminium (6061-T6) pusher plate and a z-cut sapphire window, with cavity dimensions of approximately 5 mm in diameter and 300 and 600 μm in thickness. $L\mathrm{D}_2$ samples were condensed in the cryocell by filling the cavity with high purity deuterium gas at 18 psi, cooling the cryocell to its equilibrium temperature of 16–18 K and then warming the cell to 22.0 ± 0.1 K [19]. This produced a quiescent $L\mathrm{D}_2$ sample below the boiling point of about 25 K, with nominal initial density of 0.167 g cm^{-3}.

Shock waves were generated by planar impact of either an aluminium (6061-T6) or a titanium (Ti-Al6V4) flyer plate onto the aluminium pusher plate at the front of the cryocell. The rectangular flyer plate, approximately 12×25 mm in lateral dimension and $\sim$200–300 μm in thickness[2], was accelerated across a nominal 3 mm vacuum gap by the magnetic field.

[2] The initial flyer thickness was nominally 800 μm. The $\sim$200–300 μm thickness refers to portion of the flyer at impact that remained unaffected by magnetic diffusion.

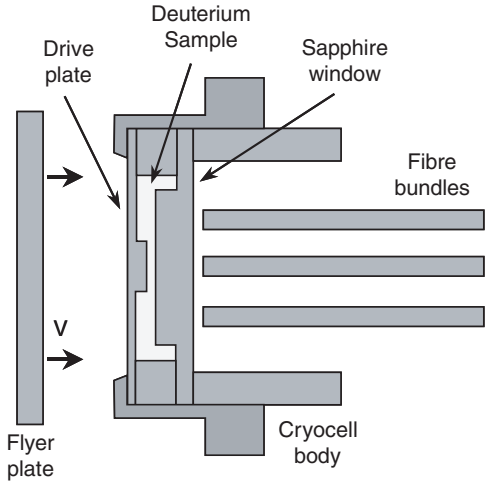

Figure 1. Experimental configuration used to obtain Hugoniot measurements in plate-impact shock wave experiments. Note the drawing is not to scale.

Titanium flyer velocities as high as ∼22 km s^{-1} have been achieved, capable of generating shock states to ∼700 GPa in the aluminium drive plate and transmitting up to ∼100 GPa shock waves into LD$_2$. Conventional velocity interferometry [20] (VISAR) was used to directly measure the velocity history of the flyer plate from launch to impact with an accuracy of ∼0.5%.

The shock response of LD$_2$ was diagnosed with a number of fibre-optic-coupled diagnostics. Typically several optical fibre bundles of 100 and 200 μm diameter fibres were used, allowing multiple, redundant diagnostics, including (i) conventional VISAR, (ii) fibre-optic shock break out (FOSBO) and (iii) temporally and spectrally resolved spectroscopy. Figure 2 shows sample data obtained from a typical LD$_2$ experiment. In all, 16 channels of data were obtained for each experiment, allowing up to 16 independent measurements of the shock velocity, U_s, in LD$_2$ and up to four independent measurements of U_s in the aluminium drive plate. The uncertainty in U_s was ∼2–3% from the measured transit time through the cell and the initial cell dimensions. Since the uncertainties were due to random errors, statistical techniques could be used to decrease the uncertainty in U_s to approximately 1% and 2% for the LD$_2$ sample and the aluminium drive plate, respectively [21].

The VISAR records for the higher pressure experiments confirm the constancy of the pressure drive obtained from the flyer plate impact, as shown in figure 2. In this case the VISAR velocity is indicative of U_s in the LD$_2$ because at shock pressures above ∼30 GPa LD$_2$ becomes reflective [3]. From these records it was determined that the shock pressure was constant to better than 1% as the shock traversed the cryocell. It is emphasized that a correction of $1/n_0$, where n_0 is the refractive index of the ambient LD$_2$, was applied to the usual velocity per fringe (VPF) constant for the interferometer to account for the diminishing thickness of LD$_2$ through which the laser light propagated as the shock front traversed the cryocell. We found that this index correction, amounting to 11.5%, was necessary to obtain consistency between U_s directly measured by the VISAR and U_s inferred from the transit time measurements.

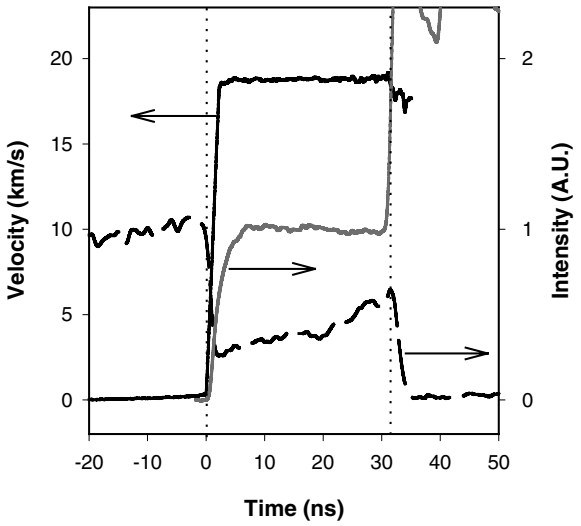

Figure 2. Typical data obtained in LD_2 experiments; (i) VISAR record of the shock front (solid line), (ii) FOSBO record (dashed line) and (iii) self-emission record (grey line). Vertical dotted lines indicated break out of the shock from the aluminium/LD_2 interface and the arrival of the shock at the LD_2/sapphire interface.

For the lower pressure experiments, the shock front was not sufficiently reflective to obtain VISAR measurements. However, U_s was obtained for all experiments using the FOSBO and self-emission data. As seen in figure 2, both of these measurements provided a clear signature of shock arrival at the aluminium/LD_2 and the LD_2/sapphire interfaces. Also, in all experiments, high quality spectra were obtained over the continuous wavelength region between 250 and 700 nm. The detailed analysis of the spectral dependence of the self-emission, which provides a measure of the temperature of the shocked LD_2, will be discussed in a future publication. We emphasize that the constancy of the emission signal during the traversal of the shock through the cryocell further verifies the constancy of the pressure states achieved with the flyer plate impact, as the intensity of emission is proportional to the pressure of the LD_2 to the $\sim$1.75 power[3].

An impedance matching method, utilizing the Hugoniot jump conditions [22], was used to obtain Hugoniot points for the shocked LD_2. As shown in figure 3, the initial shocked state of the aluminium drive plate is described in the pressure–particle velocity (P–u_p) plane by the point labelled A, and the shocked state of LD_2 is constrained to lie on a straight line, with the slope of the line given by $\rho_0 U_s$, where ρ_0 is the initial density of the LD_2 sample. An EOS model for aluminium [12] was used to calculate the release isentrope from state A in the aluminium drive plate. The intersection of the calculated release isentrope and the line defined by the LD_2 shock velocity determines u_p of the shocked deuterium sample. The uncertainty in u_p for LD_2, typically 2–3%, was determined from the uncertainty in the shocked state of the aluminium drive plate, and thus from the uncertainty in U_s for the aluminium drive plate. The density compression was then determined from the jump conditions using the expression $\rho/\rho_0 = U_s/(U_s - u_p)$.

[3] The power varies as a function of wavelength; at 400 and 600 nm the power is approximately 1.9 and 1.5, respectively.

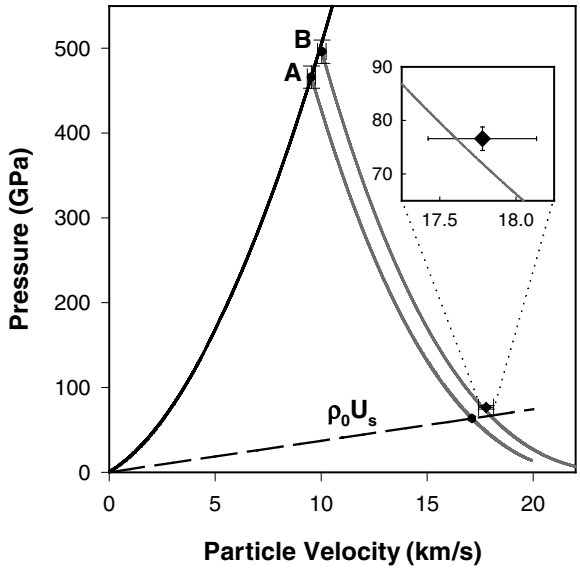

Figure 3. Impedance matching method and aluminium release measurement. Solid grey lines are calculated release isentropes from two separate experiments: state A indicates the initial shocked state of the aluminium drive plate in a $L\mathrm{D}_2$ experiment and state B indicates the initial shocked state of an aluminium sample in a silica aerogel release experiment.

The accuracy in the impedance matching technique depends upon two factors: the accuracy in the measurement of U_s in the $L\mathrm{D}_2$ and the accuracy of the calculated release isentrope for aluminium. The quality of the data shown in figure 2, and the multiplicity of the U_s measurement for each experiment, indicates that U_s in the $L\mathrm{D}_2$ is determined quite accurately. To determine the accuracy of the calculated release isentrope, release experiments in aluminium using a low density (200 mg cm^{-3}) silica aerogel were performed. This technique is similar to that used by Holmes *et al* to measure the aluminium release from ∼80 GPa [23]. Direct impact experiments were performed to generate Hugoniot data for the aerogel between 30 and 75 GPa. Experiments were then performed in which a shock was transmitted from the aluminium drive plate into the silica aerogel, which simulates unloading to the $L\mathrm{D}_2$ state. The measured U_s for the aerogel in the release experiment, along with the measured aerogel Hugoniot, determines a point in P–u_p space that the aluminium release isentrope must pass through. A typical result is shown in figure 3, in which a release point in aluminium was measured from an initial shock state of ∼500 GPa (the point labelled B in figure 3). These measurements confirm the validity of the release calculations in aluminium over the pressure range of interest, and make a strong case for the procedure indicated in figure 3 to obtain the $L\mathrm{D}_2$ Hugoniot results reported in the present work.

4. Experimental results and discussion

The pressure–density compression states determined in this way for a total of 19 experiments are displayed in figure 4. The lowest pressure experiment was found to be in good agreement with the results reported from the earlier gas-gun experiments and the lower pressure laser experiments. However, at higher pressures, particularly the data centred around 70 GPa and the data point at ∼100 GPa, there is a distinct deviation between the present results and those

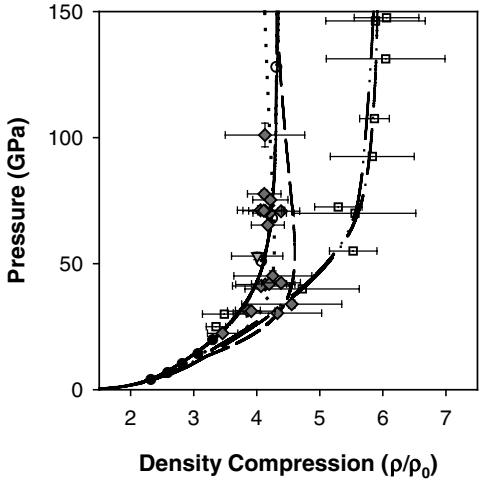

Figure 4. Deuterium Hugoniots. Theoretical models: Sesame (solid line [1]), tight binding (dotted line [4]), GGA-MD (dashed line [5]), PIMC (open circles [6]), Ross (dot-dot-dash line [7]) and Young (dot-dash line [24]). Experiments: gas-gun (filled circles [2]), laser-driven (open squares [3]), this work (grey diamonds) and convergent geometry (grey triangle [25]).

reported from the laser-driven experiments. Further, the data obtained from our study are in quite good agreement with the predictions from the *ab initio* models throughout the entire range of pressures investigated.

Also shown in figure 4 are the results of recent LD_2 Hugoniot measurements obtained using a convergent geometry technique [25]. The results, shown as a weighted average point in figure 4, appear to confirm the stiffer response observed in the present experiments. Given the fact that these experiments utilize completely independent experimental configurations, the agreement of the inferred density compression makes a strong case for a ∼4-fold limiting compression for the equilibrium response of LD_2 along the principal Hugoniot. However, there still remains a discrepancy with the inferred density from the laser-driven experiments [3].

It should be noted that both the laser technique and the magnetically driven flyer technique are new and not entirely proved, and are therefore subject to potential systematic errors. We took great pains to identify, address and minimize the potential systematic errors in the present work. In particular we assessed the constancy of the pressure drive obtained with the magnetically driven flyer through the VISAR and spectroscopy measurements, and the accuracy in the impedance matching technique through the silica aerogel experiments. Further we validated the magnetically driven flyer plate technique through aluminium symmetric impact experiments to ∼500 GPa. The results of these experiments, which will be described in a future publication, were in very good agreement with the published data on aluminium at high pressure. Finally, we have also examined potential density and pressure gradients in the flyer through improved MHD simulations [10]. The results of all these studies indicate that the experimental technique and the conclusions drawn from the measurements are internally consistent.

There are also sources of potential systematic error in the laser-driven work that centre around the diagnostic used to determine the density compression in the shocked state. The use of transverse radiography to determine the location of the shock front and the interface is a non-traditional shock diagnostic, which has not been validated on a known material.

A few potential problems associated with this type of measurement warrant discussion. First, any deviation from a constant pressure shock will result in an incorrect inference of density when using the Hugoniot jump conditions. In particular, hydrocode simulations that emulate the radiography measurements indicate that errors of up to 10–15% in the determination of density can result from modest deviations from constant pressure shocks, depending upon the pressure history. Second, it is difficult to infer velocity from a trajectory measurement to a high degree of accuracy. In particular, it was reported in the laser work that good agreement was found between the VISAR measurement of the shock front and the radiography results. However, the index correction to the VPF was not used in the analysis of the VISAR result in that study, which leads to concern regarding the accuracy of the radiography result. Finally, the pressure at which $L\mathrm{D}_2$ appears to undergo a large increase in compression in the laser results corresponds to drive pressures at which one expects the aluminium driver to melt under compression [26]. This suggests the possibility of an ill-defined interface between the aluminium drive plate and $L\mathrm{D}_2$ sample.

It has also been proposed that the laser-driven experiments may not produce an equilibrium state [27], and thus the laser results are not representative of the Hugoniot response of $L\mathrm{D}_2$. However, due to the small difference in timescale between the laser experiments and the magnetically driven flyer plate experiments (timescales differ by a factor of ∼3–7), and that the collision time is several orders of magnitude smaller than the timescales of these experiments [28], both sets of experiments are expected to reach thermodynamically equilibrium states.

It should be noted that recent laser-driven, double shock experiments have been reported as an independent confirmation to the laser-driven Hugoniot measurements [29]. Recent theoretical work [30], in which these double shock experiments are compared with *ab initio* models, shows that these experiments are not able to distinguish between the theoretical models for initial shock pressures below ∼100 GPa. Thus, there is no disagreement between the double shock experiments and the present work over the range of pressures studied. Furthermore, these are integrated experiments that depend not only on the principal Hugoniot, but also on the $L\mathrm{D}_2$ properties upon re-shock. Thus, conclusions regarding the principal Hugoniot cannot be unambiguously determined and should be viewed with caution.

As a final point, we mention that we are beginning to analyse additional data obtained from the magnetically driven flyer plate experiments that confirm ∼4-fold limiting compression for shocked $L\mathrm{D}_2$. The self-emission data obtained in the flyer plate experiments provide time of arrival of shock waves at the $L\mathrm{D}_2$/sapphire interface as the shock reverberates between the aluminium drive plate and the window. This relative timing is shown to be sensitive to the density compression due to the first shock and can be used to infer the density compression along the Hugoniot. Preliminary results, which will be discussed in detail in a future publication [31], corroborate the stiff response inferred from the impedance matching technique.

5. Conclusions

In conclusion, we have performed high-velocity plate-impact, shock wave experiments to investigate the high-pressure EOS of $L\mathrm{D}_2$. The results of these experiments are in agreement with theoretical models based upon first principles, *ab initio* methods, and corroborate the stiff shock response at pressures up to ∼100 GPa predicted by the Sesame EOS. Further, the present results disagree with earlier results reported from the laser-driven experiments at pressures above ∼40 GPa. Clearly there is a need for further theoretical and experimental work to resolve this discrepancy, and to address whether there are systematic errors in either

experimental technique, or whether there is a physical phenomenon responsible for the different response at the two differing time scales of these experiments. However, in light of the fact that both experimental techniques are new and not entirely proved, it is critical that they both be subjected to intense scrutiny.

Acknowledgments

The authors would like to thank the large team at Sandia that contributed to the design and fabrication of the flyer plate loads and cryogenic targets, and the fielding of the shock diagnostics. Sandia is a multiprogram laboratory operated by Sandia Corporation a Lockheed Martin Company, for the US DOE under contract DE-AC04-94AL8500.

References

[1] Kerley G I 1983 *Molecular Based Study of Fluids* (Washington, DC: American Chemical Society) p 107
[2] Holmes N C *et al* 1995 *Phys. Rev.* B **52** 15835
Nellis W J *et al* 1995 *Science* **269** 1249
[3] Da Silva L B *et al* 1997 *Phys. Rev. Lett.* **78** 483
Collins G W *et al* 1998 *Science* **281** 1178
[4] Lenosky T J *et al* 1997 *Phys. Rev.* B **56** 5164
Collins L *et al* 1995 *Phys. Rev.* E **52** 6202
Kwon I *et al* 1994 *Phys. Rev.* B **50** 9118
[5] Lenosky T J *et al* 2000 *Phys. Rev.* B **61** 1
[6] Militzer B and Ceperley D M 2000 *Phys. Rev. Lett.* **85** 1890
Magro W R *et al* 1996 *Phys. Rev. Lett.* **76** 1240
[7] Ross M 1998 *Phys. Rev.* B **58** 669
Ross M 1996 *Phys. Rev.* B **54** R9589
[8] Hall C A *et al* 2001 *Rev. Sci. Instrum.* **72** 1
[9] Matzen M K 1996 *Phys. Plasmas* **4** 1519
[10] Lemke R W *et al Phys. Plasmas* submitted
[11] Summers R M *et al* 1997 *Int. J. Impact Eng.* **20** 779
[12] Kerley G I 1998 *Kerley Publishing Services Report* No KPS98-1 (unpublished)
[13] Desjarlais M P 2002 Private communication
[14] Desjarlais M P 2001 *Contrib. Plasma Phys.* **41** 267
[15] Desjarlais M P, Kress J D and Collins L A 2002 *Phys. Rev.* E **66** 025401(R)
[16] Rosenthal S E, Desjarlais M P and Cochrane K R 2001 *Digest of Technical Papers, 2001 IEEE Pulsed Power Plasma Science Conference*ed R Reinovsky and M Newton (Piscataway, NJ: IEEE) p 781
[17] Seidel D B *et al* 1991 *CP90 Europhysics Conference on Computational Physics* ed A Tenner (Amsterdam: World Scientific) pp 475–82
[18] Knudson M D *et al* 2001 *Phys. Rev. Lett.* **87** 225501–1
[19] Hanson D L *et al* 2000 *Shock Compression of Condensed Matter-1999* ed M D Furnish, L C Chhabildas and R S Hixson (New York: AIP) p 1175
[20] Barker L M and Hollenbach R E 1972 *J. Appl. Phys.* **43** 4669
[21] Taylor J R 1982 *An Introduction to Error Analysis* 2nd edn (Mill Valley, CA: University Science Books) p 173
[22] Duvall G E and Graham R A 1977 *Rev. Mod. Phys.* **49** 523
[23] Holmes N C 1994 *High-Pressure Science and Technology-1993* ed S C Schmidt *et al* (New York: AIP) p 153
[24] Young D A 2002 Private communication
[25] Belov S I *et al* 2002 *JETP Lett.* **76** 433
[26] Furnish M D, Chhabildas L C and Reinhart W D 1999 *J. Impact Eng.* **23** 261
[27] Gygi F and Galli G 2002 *Phys. Rev.* B **65** 220102–1
[28] Nellis W J 2002 *Phys. Rev. Lett.* **89** 165502–1
[29] Mostovych A N *et al* 2000 *Phys. Rev. Lett.* **85** 3870
Mostovych A N 2001 *Phys. Plasmas* **8** 2281
[30] Militzer B *et al* 2001 *Phys. Rev. Lett.* **87** 275502
[31] Knudson M D *et al* 2003 *Phys. Rev. Lett.* **90** 035505–1